Int. J. Electrochem. Sci., 10 **(2015)** 1926 - 1939

International Journal of
ELECTROCHEMICAL
SCIENCE
www.electrochemsci.org

Effect of Metal Bipolar Plate Channel Fabrication on Electroplating – Using Nickel Electroplating of AISI 1045 Channel Substrate as an Example

Te-Yuan Chiang[1], *Ay-Su*[1,*], *Lin-Chang Tsai*[2], *Hung-Bin Lee*[3], *Cheng-Yu Lin*[4], *Hung-Hua Sheu*[4,*], *Cheng-Chieh Chang*[4]

[1] Department of Mechanical Engineering, Yuan-Ze University, Taiwan, ROC
[2] Department of Mechatronic, Energy, and Aerospace Engineering, Chung Cheng Institute ofTechnology, National Defense University, Taiwan, ROC
[3] Department of Materials Science and Engineering, Da-Yeh University, Taiwan, ROC
[4] Department of Chemistry & Materials Science Engineering, Chung Cheng Institute of Technology, National Defense University, Taiwan 335, ROC
[*]E-mail: shhccit@gmail.com; meaysu@saturn.yzu.edu.tw

Received: 8 December 2014 / *Accepted:* 6 January 2015 / *Published:* 19 January 2015

The surface quality is a very critical factor in the performance of the bipolar plate due to it would greatly affect the contact resistance and the corrosion resistance. In this study, results of an investigation on the effects of milling process conditions on the surface roughness and subsequent electroplating of metallic bipolar plates (BPP) for proton exchange membrane fuel cell are presented. The results of potentiodynamic polarizations show that milling parameters (feed rate and precision milling) significantly affect the corrosion behavior of bipolar plates. When the AISI 1045 steel milled at different feed rates without precision milling, the surfaces of the formed BPP channel, generally, are very rough. It results in lower corrosion resistance compared to the Ni coating on a 1045 plate. When an additional precision milling is utilized, the surface smoothness of BPP channel is improved and, thus, the corrosion current density of the Ni coated BPP channel fabricated with precision milling and the Ni coating on a 1045 plate was shown to be similar. Finally, the chromized BPP channel fabricated at a feed rate of 100 mm/s with precision milling has good corrosion resistance and interfacial contact resistance. Both satisfy the Department of Energy‘s (DOE) goal for BPP application. The result can serve as reference for future research on channel fabrication.

Keywords: fuel cell; metal bipolar plate; channel milling; nickel electroplating

1. INTRODUCTION

High efficiency and low pollution alternative energy has become a topical subject around the world, and the high-performance fuel cell is one of the focuses in green energy research. The Proton Exchange Membrane Fuel Cell (PEMFC), which uses solid electrolyte as the medium of proton transfer, is characterized by low working temperature, quick start, high conversion efficiency, simple structure, noise free operation, pollution-free emissions, low heat source, high energy density, high reliability, and extensive applications. Thus, it has become the new generation of alternative energy.

The main function of bipolar plates (BPPs) is to transfer battery current and fuel gas. The gas flows evenly through the gas channel to the gas diffusion layer, while the anode and cathode conduct electrons and heat in the reaction process. Therefore, BPPs must have superior mechanical properties, good electrical, thermal conductivity, and gas tightness, in order to perform PEMFC system functions [1-3]. The acid circuit should have corrosion resistance, chemical stability, and good heat endurance when combined with other battery assemblies. The BPPs production and assembly cost is about 30~45% of the total battery cost [4]. At present, fuel cell BPPs is mostly made of graphite material, which is a good electrode material due to its low resistance and corrosion resistance. It generates high battery output power, and has stable physical and chemical properties without deterioration. However, due to its brittleness and poor mechanical properties, it is difficult to mechanically process the gas channel, as the battery may crack during assembly. This restricts the application of the battery, the cost is increased, and bulk production is difficult [5]. The metal is characterized by good ductility, electrical conductivity, machinability, airtightness, and low cost. It can remedy the defects of the traditional graphite bipolar plate, reducing the cost and volume of BPPs. The corrosion resistance of a metal bipolar plate is a problem to be solved in the development, as it may poison the proton exchange membrane [6,7] and reduce battery performance [8,9]. Therefore, a metal finishing technique is used to enhance the corrosion resistance and stability of BPPs. At present, BPP substrates can be divided into three types, namely iron-base alloy, nickel-base alloy, aluminum, and titanium light metals. The surface treatment processes include evaporation, sputtering, electroplating, chemical vapor deposition, and pack chromization.

Nickel electroplating is characterized by good corrosion resistance and attrition resistance protecting substrate. As the nickel electroplating solution system, plating solution composition, and operating conditions have been well developed, the nickel electroplating process is extensively used in material surface treatment. In the hyperthermic treatment of iron-based material, especially carbon steel material, nickel electroplating forms a good barrier layer, which buffers the diffusion of iron atoms to the surface layer and reduces the formation of ferric oxide, resulting in good treatment outcome for improving the corrosion resistance and electrical conductivity of the specimen [10-12].

Metal BPPs have good electrical conductivity, high mechanical strength, high power density, and easy machine shaping. At present, the common materials include stainless steel [13,14], aluminum alloys [15], and titanium alloys [16]. This study used AISI 1045 carbon steel as the BPP substrate for the consideration of efficient cost reduction. As the corrosion resistance of BPPs is mainly in the surface layer, the same goal can be attained by correct treatment. The iron-base material, as based on carbon steel, has relative advantage in relative cost performance. Previous studies [17-21] used iron-

base material, pretreatment, and low temperature pack chromization. There are abundant results to prove the feasibility of using low cost iron-base material to make BPPs.

This study discussed the nickel electroplating process of the AISI 1045 carbon steel specimen with a milling channel in order to determine the influence of channel processing on the electroplating operation, thus facilitating the evaluation of the differences between flat samples and channel samples. The result showed that electroplating and low temperature pack chromization can enhance surface corrosion resistance, thus, the appropriate process can be determined for mass production of light or miniature BPPs.

2. EXPERIMENTAL METHOD

2.1 Sample preparation

The AISI 1045 carbon steel with chemical composition as shown in Table 1 was used as the substrate in this experiment. Specimens were cut into the dimensions of 40mm×40mm×2mm. The surface of the 1045 steel was polished by using silicon carbide abrasive paper up to 800#, soaked in acetone or alcohol, and placed in an ultrasonic oscillator to remove the surface oil and fat. Finally, it was dried by nitrogen for future use.

Table 1. Chemical composition of AISI 1045 carbon steel

Elements	C	Cu	Mn	P	Fe
wt(%)	0.4-0.5	<0.25	<0.7	<0.01	Balance

The fabrication of channel was carried out on a Machining Center (MC) with a ball-end carbide mill. The ball-end mill used had a radius of 1 mm. The spindle speed was fixed at 8000 rpm. The feed rates were set as 50, 75, 100, 125, 150, and 175 mm/min. The depth of cut was 1mm, and cut through six passes. To fully investigate the influence of the fabrication parameters on the surface morphology and the subsequent electroplating, the milling was performed with or without finish milling to form channels from different processing conditions. The finish milling was carried out by reducing the depth of cut to 0.5 mm in the last pass of milling. Due to numerous defects existed on the milled surfaces and ultrahigh residual stress inside the channel, the formed samples were placed into the oil bath immediately to prevent the samples being corroded in the atmospheric environment. Before electroplating process, the surface oil and fat were removed with alkali in an ultrasonic cleaner for 5 min.

2.2 Nickel electroplating and low temperature pack chromization

Before pack cementation, substrate was pretreated by Ni electroplating to activate the surface. The Ni layer was deposited from a nickel sulphamate-based electrolyte. The composition of the

electroplating bath is listed in Table 2. The Ni electroplating was carried out for 30 min with the conditions of 2.5 ASD, room temperature, stirring rate of 100 rpm, and pH of 3.0.

The pack chromization was carried out following the method described in our previous study [10]. The pack powder used as chromizing deposition is a mixture of metallic chromium (Cr), halide activator (NH_4Cl), and inactive filler (Al_2O_3) in a proper ratio. The prepared sample was immersed in the powder, and placed in a furnace with argon to prevent the sample from oxidizing during the pack chromization. Pack chromization involved two heating stages.

Table 2. Composition of nickel electroplating bath

Constituents	g/L
$Ni(NH_2SO_3)_2$	450g
H_3BO_3	30g
DI water	To 1L

In Stage 1, the temperature was increased at 10℃/min to 150℃, which was maintained for 30 min, and the water vapor in the pack chromization furnace was removed by baking. In Stage 2, the temperature was increased at 10℃/min to an appropriate diffusion temperature, which was 800℃ in this experiment. The temperature was maintained for 2 h, and reduced to room temperature before the sample was removed.

2.3 Coating structure property and composition analysis

The surface and cross-sectional images of the samples were observed using scanning electron microscopy (SEM). The sample was mounted and polished before micro etching in order to observe coating thickness and overall uniformity of the coating. The crystalline structures and constituent phases of the coatings were examined by X-ray diffraction (XRD) with Cu Kα radiation (λ = 0.15405 nm) over a scanning range from 30^o to 70^o.

2.4 Electrochemical tests

To measure the corrosion resistance, potentiodynamic tests were carried out in a typical three-electrode cell system in which a platinum sheet acted as the counter electrode, an Ag/AgCl electrode (197 mV vs. SHE) as the reference electrode and the tested specimens as the working electrode. A 0.5M H_2SO_4 solution at room temperature was used as the electrolyte to simulate the environment simulating of PEMFC. All experiments were conducted in an Autolab PGSTAT30 potentiostat/galvanostat controlled by the GPES (General Purpose Electrochemical System) software. The linear polarization curves were measured in the potential range between −0.5 V and 0.8 V referred

to open circuit potential, with a scanning rate of 0.5 mV s^{-1}. The polarization curve of the sample was obtained by recording the voltage or current value during the experiment. When potentiostatic tests were performed, the 0.6V (vs. SCE) potential with air purging was applied to simulate the cathodic environment in a 0.5 M H_2SO_4 solution at 80 ◦C for 1 h.

3. RESULTS AND DISCUSSION

3.1 Coating microstructure

The surface roughness greatly varies with the change of milling process parameters. Figure 1 depicts the surface morphology of nickel films deposited on the bottom surface of the BPP channels fabricated at different feed rates without precision milling. Scratches resulted from milling appearing in surface were clearly observed in the channels fabricated without precision milling. The scratches were not covered completely even after nickel electroplating. When a precision milling is used, however, the scratches inside the channel were markedly reduced, and the Ni deposits were uniformly coated on the surfaces (Fig. 2).

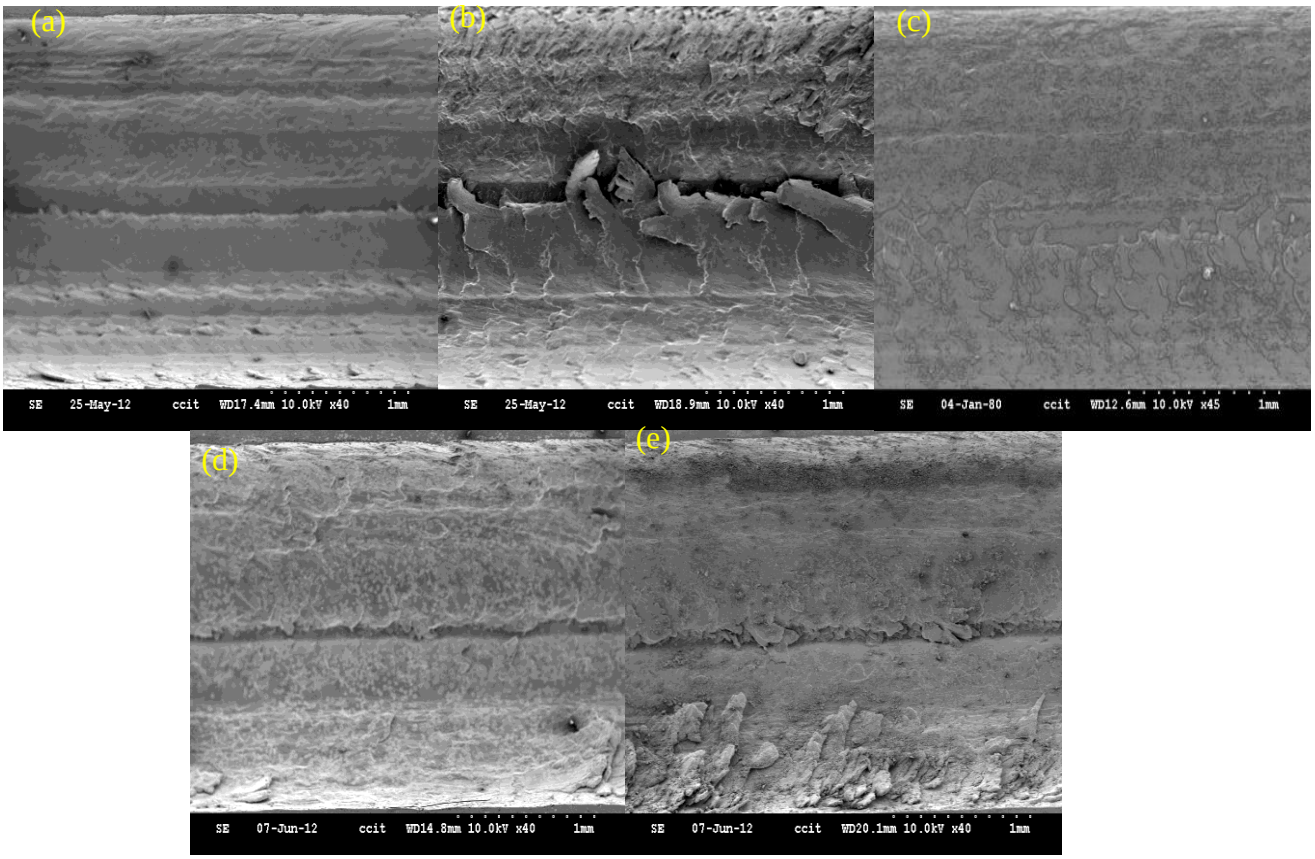

Figure 1. SEM micrograph of the surface of the Ni coated BPP channel fabricated at different feed rates without precision milling: (a) 50 mm/min (b) 75 mm/min (c) 100 mm/min (d) 150 mm/min (e) 175 mm/min.

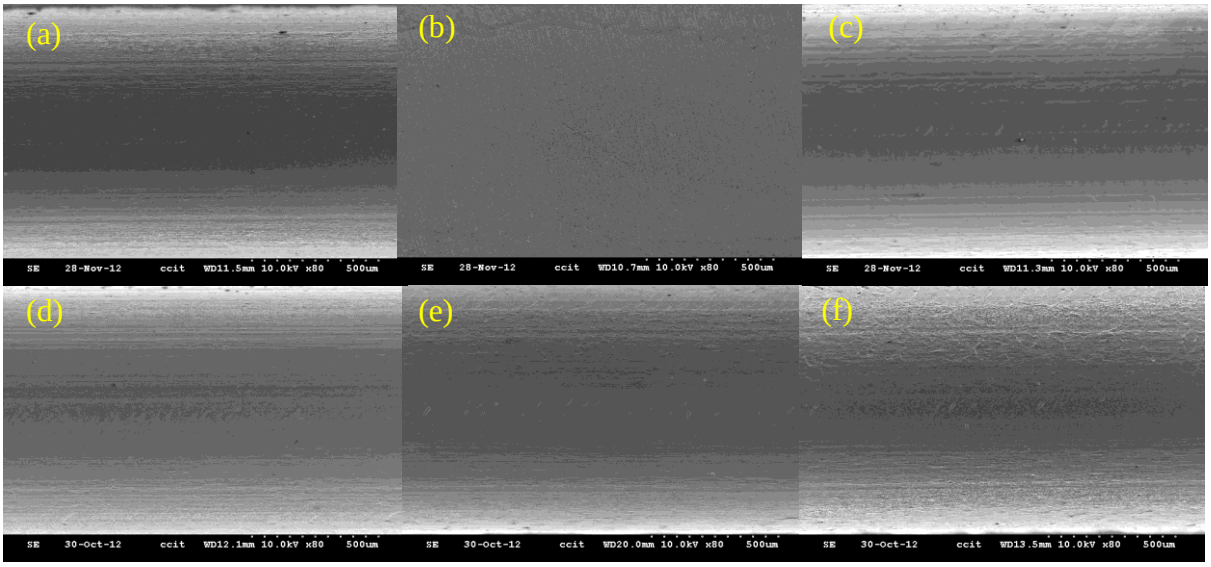

Figure 2. SEM micrograph of the surface of the Ni coated BPP channel fabricated at different feed rates with precision milling: (a) 50 mm/min, (b) 75 mm/min, (c) 100 mm/min, (d) 150 mm/min, (e) 175 mm/min.

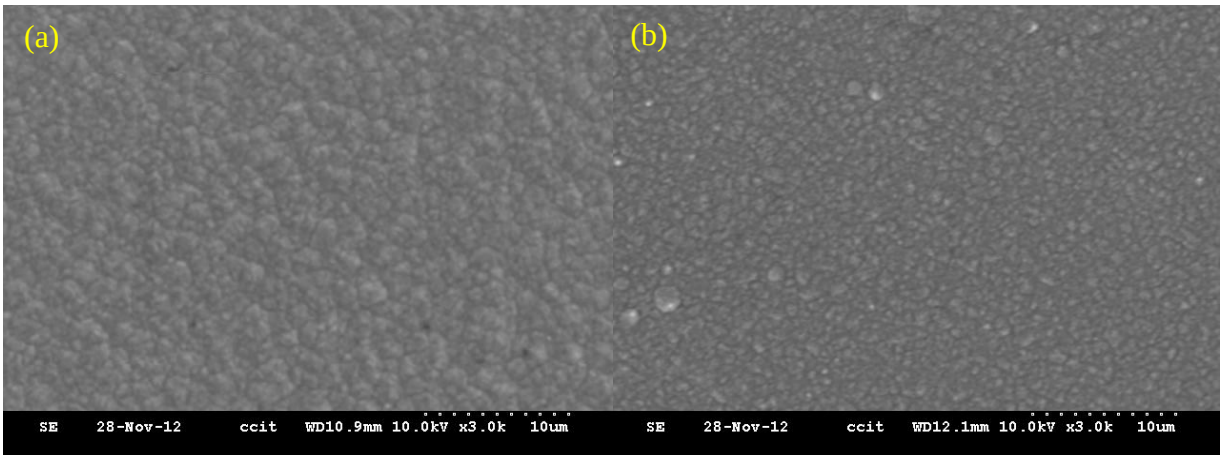

Figure 3. SEM micrograph of (a) plane part, and (b) concave part of surface for the Ni coated BPP channel fabricated at 100 mm/min with precision milling.

Fig. 3 illustrates the influence of the surface topography on the grain size of nickel coatings obtained at plane and concave parts of the BPP channel milled at the feed rate of 100 mm/min. It can be clearly seen that both coatings were formed of globular grains, with typical sizes of 0.5–1.5 μm. However, the grain size of nickel crystallites on concave part is smaller than that of plane part. The results obtained suggest that for crystallite sizes may be explained in terms of surface roughness. Higher surface roughness of concave part, as shown by the existence of some fine scratches on the sample, promotes nucleation and, thus, reduction of the grain size. Similar results were observed when the milling was carried out at different feed rates. Therefore, only the results utilized a feed rate of 100 mm/min were displayed in further study.

Cross-sections of the electrodeposited nickel film are presented in Fig. 4. It is observed in Fig. 4 that the Ni layer was uniformly and continuously coated on the channel surface, which filled the scratches inside the channel to protect the substrate.

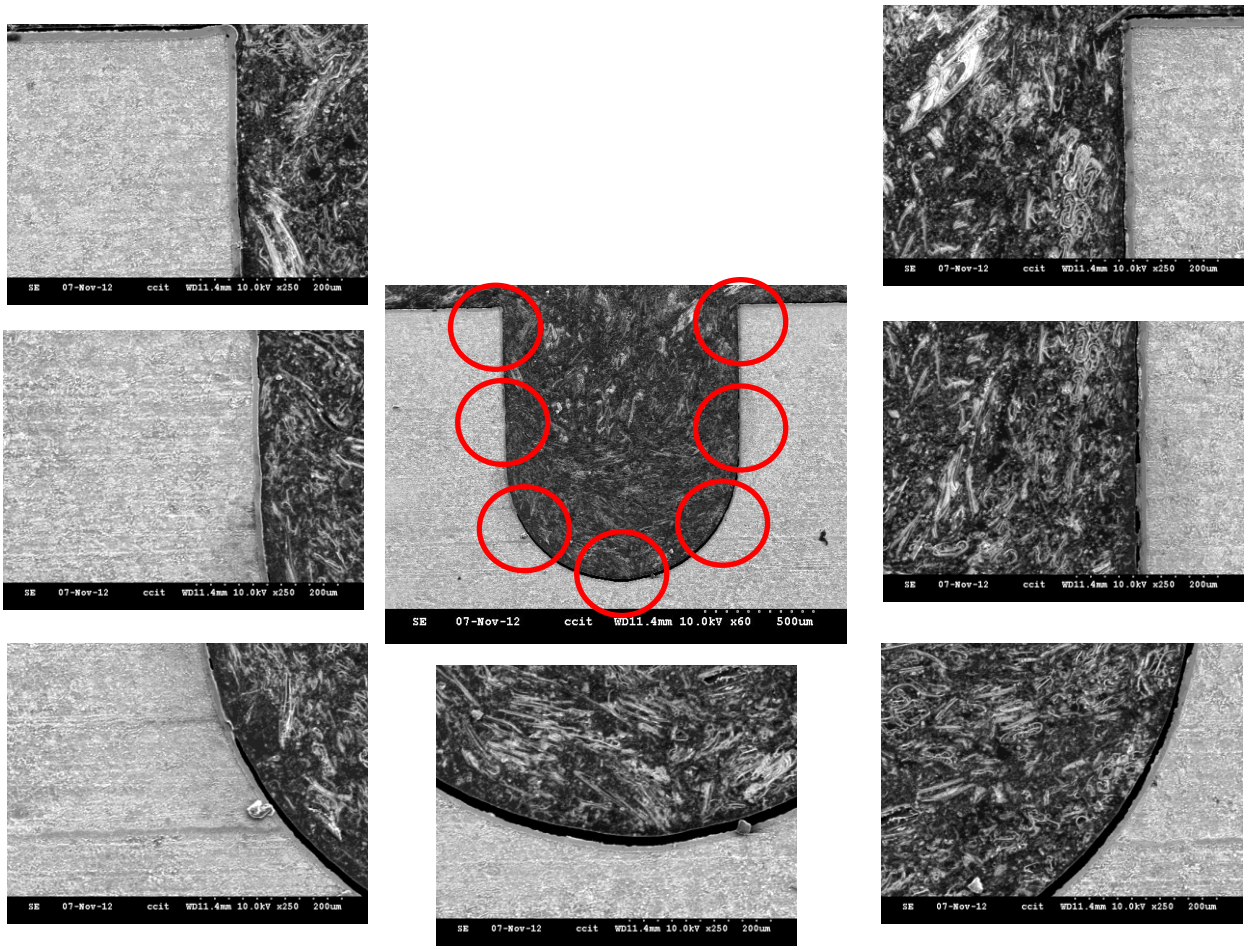

Figure 4. The cross-sectional SEM image of the Ni coated BPP channel milled at a feed rate of 100mm/min with precision milling.

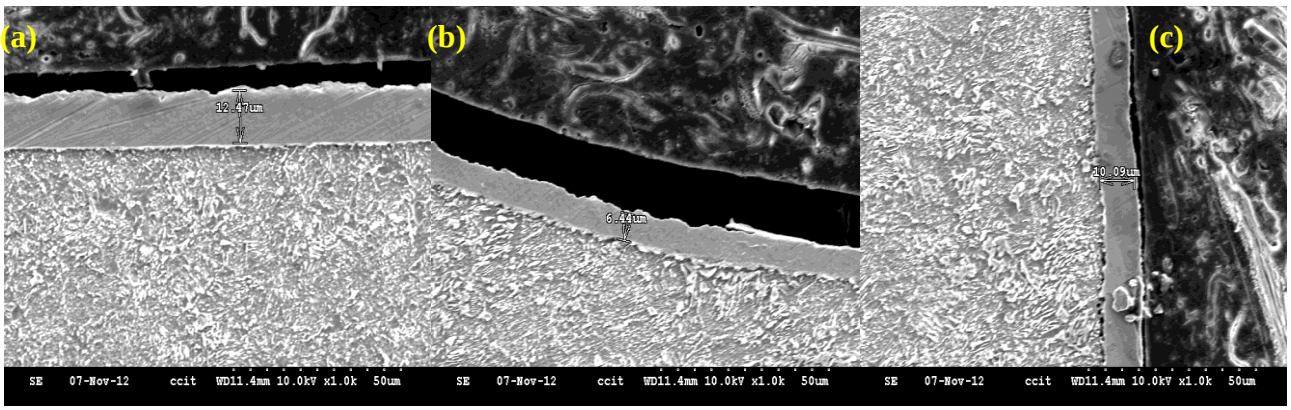

Figure 5. The cross-sectional SEM image of (a) plane, (b) bottom, and (c) side for the Ni coated BPP channel milled at a feed rate of 100mm/min with precision milling.

Moreover, the Ni layer showed very compact and no pores from its cross-section observation, which would be expected to greatly improve its corrosion resistance. When examining the cross sectional SEM micrographs of the different surfaces on the same nickel coated bipolar plate channel (Fig. 5), it is evident that the thickness of nickel coating decreases with the increase of distance to the anode. The plane coating thickness was 12 μm, the side coating thickness was 10 μm, and the bottom coating thickness was 6 μm. The thickness of coating decreases from the plate surface to the channel bottom.

The corresponding XRD spectrum for the resultant electroplated coating is shown in Fig. 6. Two characteristic peaks for nickel (2θ ~44.5 and 51.8), marked by their indices ((111) and (200)) were observed. Accordingly, it could be concluded that the Ni layer prepared in this work were of pure nickel.

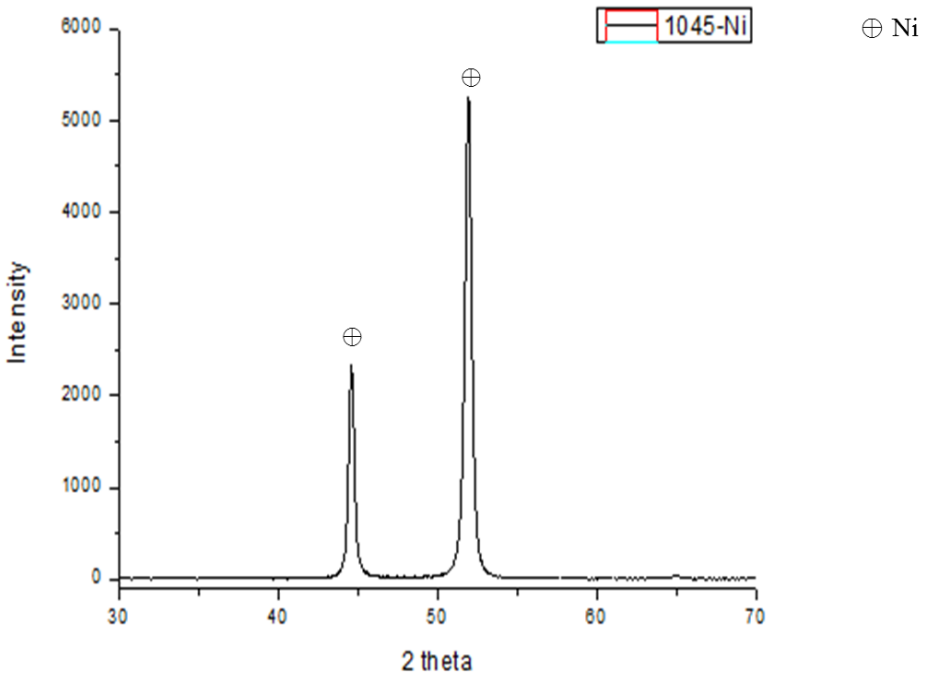

Figure 6. X-ray diffraction pattern of nickel coated BPP fabricated at a feed rate of 100mm/min with precision milling.

3.2 Potentiodynamic test results of Ni coatings on BPP channels

Fig. 7 shows potentiodynamic polarization curves for Ni coated BPP channels fabricated without precision milling in a 0.5 M H_2SO_4 solution at room temperature.

The corrosion current density (I_{corr}) and corrosion potential (E_{corr}) are calculated from the intercept of the anodic Tafel slope β_a and cathodic Tafel slope β_c, and are given in Table 3. Uncoated 1045 steel was also included in the experiments for comparison purposes. The polarization curves of the Ni coated 1045 stainless steel shows a lower corrosion current density (I_{corr}) of 6.37×10^{-5} Acm^{-2} than bare 1045 stainless steel (3.75×10^{-3} Acm^{-2}), suggesting that the Ni coating can improve the corrosion resistance.

Table 3. I_{corr} and E_{corr} measured in a 0.5M H_2SO_4 solution at room temperature for bare 1045 steel and Ni coated BPP samples fabricated without precision milling

Substrate-rough milling feed rate (mm/s)-coating	βa (V/ decade)	βc (V/ decade)	I_{corr}(A/cm^2)	E_{corr}(V)
1045	8.13	-8.82	3.75×10^{-3}	-0.445
1045-Ni	156.71	-681.22	6.37×10^{-5}	-0.245
1045-F50R-Ni	62.30	-157.80	2.14×10^{-4}	-0.268
1045-F75R-Ni	43.60	-168.95	2.62×10^{-4}	-0.292
1045-F100R-Ni	519.48	-487.80	3.97×10^{-5}	-0.303
1045-F150R-Ni	72.4	-474.16	1.34×10^{-4}	-0.231
1045-F175R-Ni	32.80	-138.24	1.82×10^{-4}	-0.183

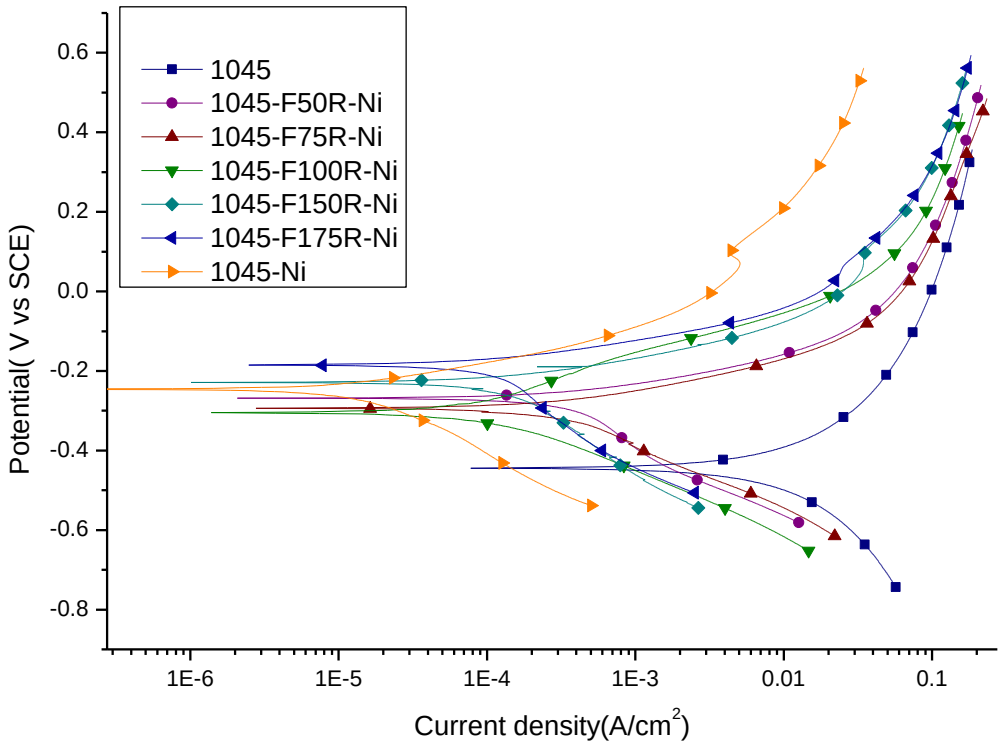

Figure 7. Polarization curves measured in a 0.5M H_2SO_4 solution at room temperature for bare, Ni coated 1045 steel and various Ni coated BPP channels fabricated without precision milling.

On the other hand, it can be clearly seen from Table 3 that the corrosion current density of Ni coated BPP channels fabricated with rough milling are higher than that of the Ni coated 1045 steel without milling except in the case of Ni coated specimen milled at 100 mm/s. Meanwhile, the corrosion potential E_{corr} of all Ni coated BPP channels fabricated with rough milling shift to negative direction by contrast to the un-milled one. This result suggests that rough milling would deteriorate the corrosion resistance of the Ni coated samples. This can be attributed to an increased extent of scratches, which not only lead to an increase in surface roughness but also affect the complete

coverage of Ni coating. As shown in Fig. 1, the surface of Ni coated BPP channels fabricated with a milling feed rate of 100 mm/s is smoothest, thus, sample 1045-F100R-Ni shows it has lowest corrosion current density (3.97×10^{-5}).

Table 4. I_{corr} and E_{corr} measured in a 0.5M H_2SO_4 solution at room temperature for Ni coated BPP samples fabricated with precision milling

Substrate-rough and precision milling feed rate (mm/s) -coating	βa (V/ decade)	βc (V/ decade)	I_{corr}(A/cm^2)	E_{corr}(V)
1045-F50F-Ni	88.70	-114.06	9.72×10^{-5}	-0.295
1045-F75F-Ni	336.42	-442.20	3.92×10^{-5}	-0.290
1045-F100F-Ni	274.72	-363.32	3.72×10^{-5}	-0.295
1045-F125F-Ni	258.33	-212.76	2.58×10^{-5}	-0.312
1045-F150F-Ni	184.87	-206.18	2.35×10^{-5}	-0.300
1045-F175F-Ni	358.74	-466.32	2.27×10^{-5}	-0.304

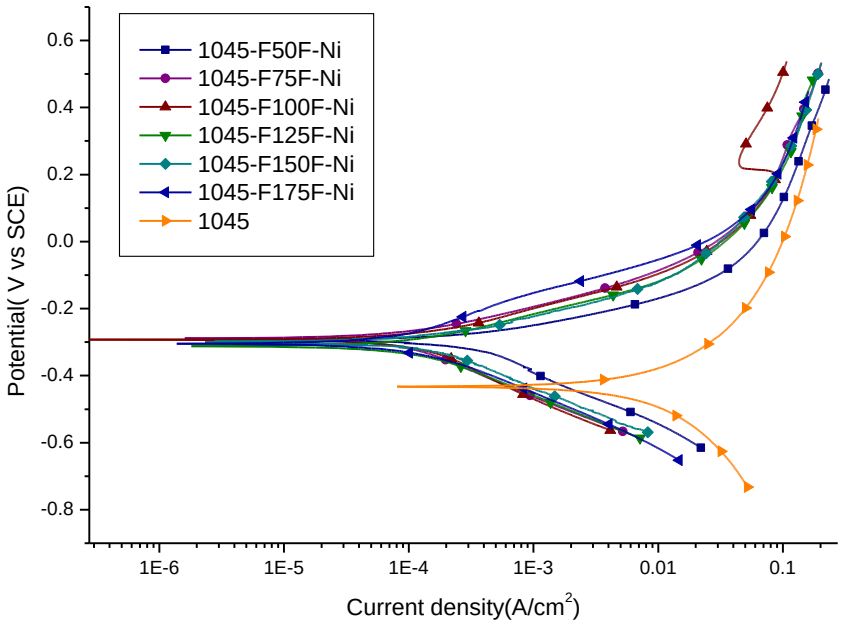

Figure 8. Polarization curves measured in a 0.5M H_2SO_4 solution at room temperature for bare 1045 steel and various Ni coated BPP channels fabricated with precision milling.

SEM micrographs of Ni coatings on surface with different milling (Fig.1 and Fig. 2) clearly demonstrated that the morphologies of Ni coatings were visually different. The extent of surface roughness significantly reduced as a precision milling step was performed. Improved corrosion resistance can be expected for these Ni coated BPP channels fabricated with precision milling due to their smoother surfaces which having fewer flaws and defects. The potentiodynamic polarization curves for Ni coated BPP channels fabricated with precision milling in a 0.5 M H_2SO_4 solution at room

temperature are shown in Fig. 8. Their corresponding corrosion current densities, corrosion potentials, anodic Tafel slope β_a and cathodic Tafel slope β_c are listed in Table 4. The i_{corr} decreased with an increase of the precision milling feed rate. One may see from the result of Table 4 that the corrosion resistance increased with an increase in smoothness. The result is consistent with the literature report [22] which shows that the corrosion resistance can be improved by smoothing the surface.

3.3 Effect of low temperature pack chromization

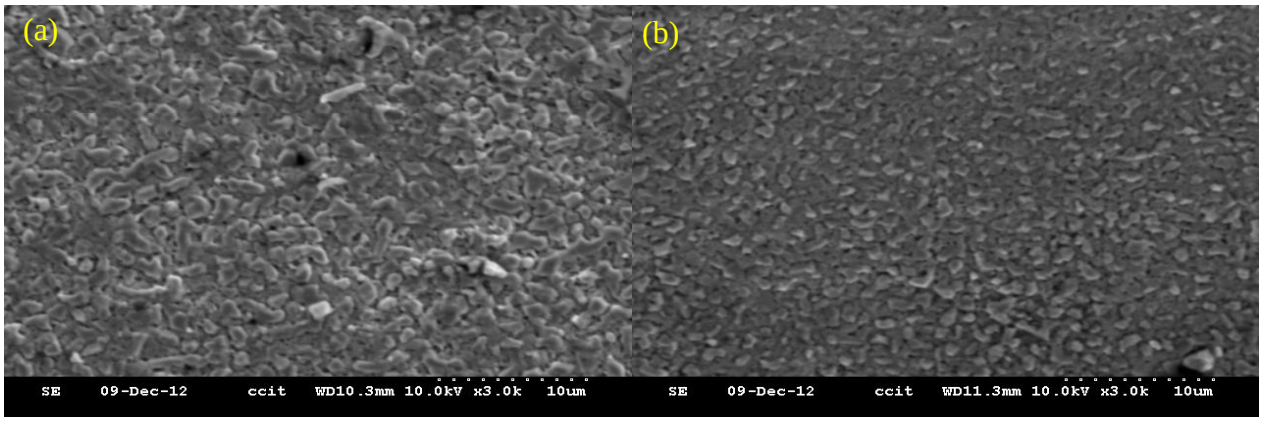

Figure 9. SEM micrograph of (a) plane part, and (b) concave part of surface for the chromized BPP channel fabricated at 100 mm/min with precision milling.

Pack chromization is one of the easiest and cheapest processes to obtain the chromizing coatings to improve the corrosion resistance, hardness, and weariness of various carbon steels [23, 24]. Unfortunately, the pack cementation was normally performed at temperatures above 1000 ℃, which has a detrimental effect on the mechanical properties of work pieces.

Therefore, reducing pack-cementation temperature is required for widespread application of the chromizing coatings. Generally, the operation temperature can be decreased by activating the surface of the base metal [25]. In previous study [25] has shown that electroplating of Ni is an effective method to activate the stainless steel for subsequent pack chromization. To prevent the diffusion of iron atoms from the substrate to the surface layer during the chromization process and produce a homogeneous as well as continuous chromium coating, therefore, the low temperature pack chromization was only performed on the Ni coated BPP samples fabricated with precision milling. Surface morphologies of specimen 1045-F100F-Ni-Cr(800-2) chromized at 800 ℃ for 2 h are shown in Fig. 9. It shows from Fig. 9 that a compact and continuous chromized layer was deposited on both plane and bottom parts of BPP channel fabricated at feed rate of 100 mm/s with precision milling.

The potentiodynamic polarization curves of chromized coating, Ni coated 1045 steel and raw 1045 steel tested in a 0.5 M H_2SO_4 solution at 25℃ are shown in Fig. 10. The corresponding corrosion parameters, including corrosion potential, corrosion current density, anodic Tafel slope β_a and cathodic Tafel slope β_c are listed in Table 5.

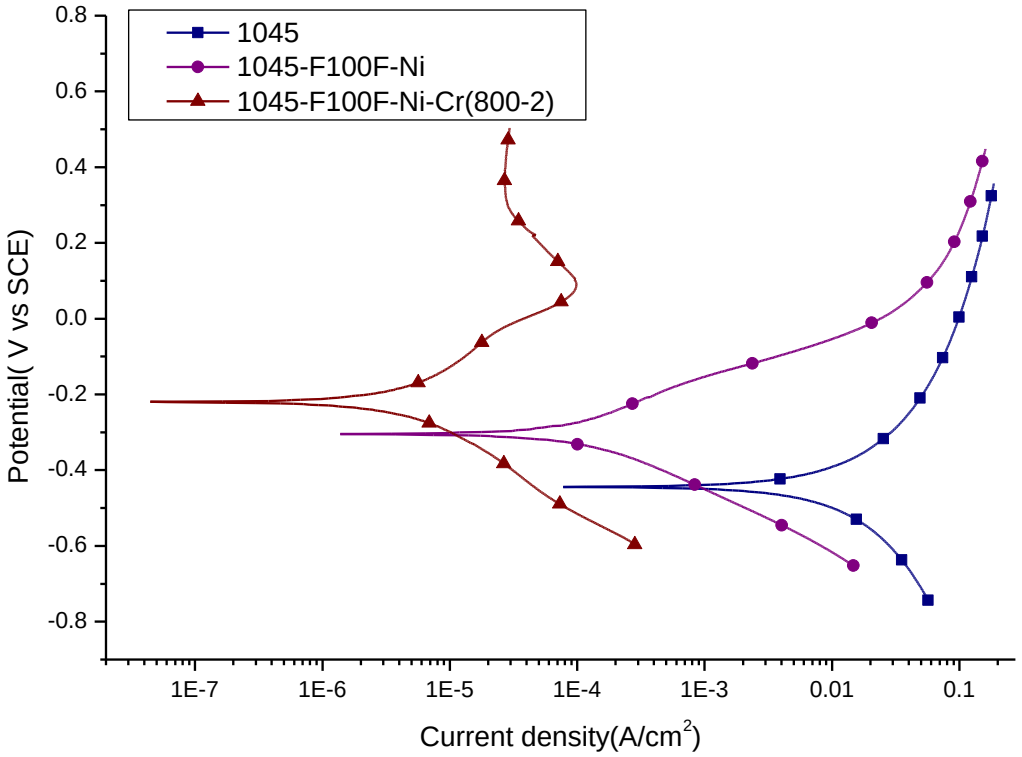

Figure 10. Polarization curves measured in a 0.5M H_2SO_4 solution at room temperature for bare 1045 steel, Ni coated BPP channel, and chromized BPP channel.

Table 5. I_{corr} and E_{corr} measured in a 0.5M H_2SO_4 solution at room temperature for bare 1045 steel, Ni coated BPP sample and chromized BPP sample

Substrate-rough and precision milling feed rate (mm/s) –coating1-coating2	βa (V/ decade)	βc (V/ decade)	I_{corr}(A/cm^2)	E_{corr}(V)
1045	8.13	-8.82	3.75×10^{-3}	-0.445
1045-F100F-Ni	470.10	-471.15	3.72×10^{-5}	-0.304
1045-F100F-Ni-Cr(800-2)	16333.33	-11340.20	1.67×10^{-6}	-0.219

The polarization curves of Ni coated 1045 steel and raw 1045 steel are almost free of active-passive transition, while the chromized 1045 steel shows a typical polarization curve of passive metals. It is clear from Fig. 10 that the corrosion potential of chromized sample is higher than that of the substrate and Ni coated specimen, but the corrosion current density is much lower, indicating that the corrosion resistance of the 1045 steel is obviously modified by chromization process based on the analyses of polarization curves. This result can be further confirmed from Table 5. Additionally, the contact resistance was 8 mΩ×cm^2 under the compressive stress of 140 N/cm^2, which met the commercial specifications of the fuel cells of the United States Department of Energy (DOE).

4. CONCLUSION

The effect of milling process parameters on surface roughness of AISI 1045 steel BPPs was investigated. Our results showed that feed rate is highly responsible for the surface roughness. The BPP channel fabricated without precision milling resulted in more scratches and plastic deformation. Even after nickel electroplating, the scratches were still visible. Ni coated BPP channel fabricated without precision milling resulted in lower corrosion resistance compared to the Ni coating on a 1045 plate. Nevertheless, all the corrosion resistances acquired for the Ni coated BPP channel fabricated with precision milling were extremely improved. The corrosion current density of the Ni coated BPP channel fabricated with precision milling and the Ni coating on a 1045 plate was shown to be similar. It indicates that an additional precision milling procedure could effectively increase the surface smoothness and, thus, reduce the influence of the milling feed rate on electroplating. The polarization curve measured in a 0.5 M H_2SO_4 solution at room temperature showed that the corrosion resistance of the BPP channel was dramatically improved after low temperature pack chromization. Both corrosion current density and ICR value of chromized sample meets the U.S. DOE target for bipolar plate application.

References

1. H. Wang, M.A. Sweikart and J.A. Turner, *Journal of Power Sources*, 115 (2003) 243.
2. R.A. Antunes, M.C.L. Oliveira, G. Ett and V. Ett, *Int. J. Hydrogen Energy*, 35 (2010) 3632.
3. J. André, L. Antoni and J.P. Petit, *Int. J. Hydrogen Energy*, 35 (2010) 3684.
4. S.J. Lee, C.H. Huang, J.J. Lai, and Y.P. Chen, *Journal of Power Sources*, 131 (2003) 243.
5. R.C. Makkus and H.H. Janssen, *Fuel Cells Bulletin*, 3 (2000) 5.
6. T. Chaudhuri, A. Hermann and P. Spagnol, *Int. J. Hydrogen Energy*, 30 (2005) 1297.
7. H. Tawfik, Y. Hung and D. Mahajan, *Journal of Power Sources*, 163 (2007) 755.
8. R. Jiang and D. Chu, *Journal of Power Sources*, 93 (2001) 25.
9. A. Pozio, R.F. Silva, M.D. Francesco and L. Giorgi, *Electrochim. Acta*, 48 (2003) 1543.
10. K.S. Weil, J.Y. Kim, G. Xia, J. Coleman and Z.G. Yang, *Surf. Coat. Technol.*, 201 (2006) 4436.
11. H. Wang, M.P. Brady, G. Teeter and J.A. Turner, *Journal of Power Sources*, 138 (2004) 86.
12. P. Niranatlumpong and H. Koiprasert, *Surf. Coat. Technol.*, 201 (2006) 737.
13. N.D. Heras, E.P.L. Roberts, R. Langton and D. Hodgson, *Energy & Environmental Sciences*, 2 (2009) 206.
14. T.M. Wen, K.H. Hou, C.Y. Bai, M.D. Ger, P.H. Chien and S.J. Lee, *Corros. Sci.*, 52 (2010) 3599.
15. K.S. Eom, M. Kim, S.K. Oh, E.A. Cho and H.S. Kwona, *Int. J. Hydrogen Energy*, 36 (2011) 11825.
16. S.H. Wang, J.C. Peng, W.B. Lui and J.S. Zhang, *Journal of Power Sources*, 162 (2006) 486.
17. L.C. Tsai, H.H. Sheu, C.C. Chen and M.D. Ger, *Int. J. Electrochem. Sci.*, 10 (2015) 317.
18. C.Y. Bai, J.L. Lee, T.M. Wen, K.H. Hou, M.S. Wu and M.D. Ger, *Appl. Surf. Sci.*, 257 (2011) 3529.
19. C.Y. Bai, T.M. Wen, K.H. Hou, N.W. Pu and M.D. Ger, *Int. J. Hydrogen Energy*, 36(2011) 3975.
20. H.C. Wang, K.H. Hou, C.E. Lu and M.D. Ger, *Thin Solid Films*, 570 (2014) 209.
21. C.Y. Bai, T.M. Wen, M.S. Huang, K.H. Hou, M.D. Ger and S.J. Lee, *Journal of Power Sources*, 195(2010) 5686.
22. X.Y. Wang, Y.S. Wu, L. Zhang and Z.Y. Yu, *Corros.*, 57 (2001) 540.
23. C.Y. Wei, F.S. Chen, *Mater. Chem. Phys.*, 91 (2005) 192.

24. L. Levin, A. Ginzburge, L. Klinger, T. Werber, A. Katsman and P. Schaaf, *Surf. Coat. Technol.*, 106 (1998) 209.
25. Z.B. Wang, J. Lu and K. Lu, *Acta Mater.*, 53 (2005) 2081.